

Large-scale structure and hyperuniformity of amorphous ices

Fausto Martelli¹, Salvatore Torquato^{1,2}, Nicolas Giovambattista^{3,4}, Roberto Car^{1,2}

¹*Department of Chemistry, Princeton University, Princeton NJ, USA*

²*Department of Physics, Princeton University, Princeton NJ, USA*

³*Department of Physics, Brooklyn College of the City University of New York, New York, NY, USA*

⁴*Ph.D. Programs in Chemistry and Physics, The Graduate Center of the City University of New York, New York, New York 10016, USA*

We investigate the large-scale structure of amorphous ices and transitions between their different forms by quantifying their large-scale density fluctuations. Specifically, we simulate the isothermal compression of low-density amorphous ice (LDA) and hexagonal ice to produce high-density amorphous ice (HDA). Both HDA and LDA are nearly hyperuniform, i.e., they are characterized by an anomalous suppression of large-scale density fluctuations. By contrast, in correspondence with the non-equilibrium phase transitions to HDA, the presence of structural heterogeneities strongly suppresses the hyperuniformity and the system becomes hyposurficial (devoid of "surface-area fluctuations"). Our investigation challenges the largely accepted "frozen-liquid" picture, which views glasses as structurally arrested liquids. Beyond implications for water, our findings enrich our understanding of pressure induced structural transformations in glasses.

Introduction.— Disordered hyperuniform materials are exotic amorphous states of matter that lie between a crystal and a liquid: they are like perfect crystals in the way they suppress large-scale density fluctuations and are like liquids or glasses in that they are statistically isotropic with no Bragg peaks [1]. Central to the concept of hyperuniformity is the structure factor $S(\mathbf{k})$ which, in the thermodynamic limit, is related to $\tilde{h}(\mathbf{k})$, the Fourier transform of the total correlation function $h(\mathbf{r})$, $S(\mathbf{k}) = 1 + \rho\tilde{h}(\mathbf{k})$. In d -dimensional Euclidean space, \mathbb{R}^d ($d = 3$ in this work), the number variance $\sigma^2(R)$ of particles inside a spherical window of radius R is related to $S(\mathbf{k})$ via [1]:

$$\sigma^2(R) = \langle N(R) \rangle \left[\frac{1}{(2\pi)^d} \int_{\mathbb{R}^d} S(\mathbf{k}) \tilde{\alpha}(\mathbf{k}; R) d\mathbf{k} \right] \quad (1)$$

where $\langle N(R) \rangle$ is the average number of particles inside the spherical window and $\tilde{\alpha}(\mathbf{k}; R)$ is the Fourier transform of $\alpha(\mathbf{r}; R)$, defined as the volume common to two spherical windows with centers separated by a vector \mathbf{r} , divided by the volume of the window. For a large class of ordered and disordered systems, the number variance has the following large- R asymptotic behavior [1, 2]:

$$\sigma^2(R) = 2^d \phi \left[A \left(\frac{R}{D} \right)^d + B \left(\frac{R}{D} \right)^{d-1} + \ell \left(\frac{R}{D} \right)^{d-1} \right] \quad (2)$$

where $\phi = \rho v_1(D/2)$ is the dimensionless density, D is a characteristic length, $v_1(R)$ is the volume of the spherical window, A and B are "volume" and "surface-area" coefficients, respectively, while $\ell(R/D)^{d-1}$ represents terms of lower order than $(R/D)^{d-1}$. A and B can be expressed as:

$$A = \lim_{|\mathbf{k}| \rightarrow 0} S(\mathbf{k}) = 1 + d2^d \phi \langle x^{d-1} \rangle \quad (3)$$

and

$$B = - \frac{d^2 2^{d-1} \Gamma(\frac{d}{2})}{\Gamma(\frac{d+1}{2}) \Gamma(\frac{1}{2})} \phi \langle x^d \rangle \quad (4)$$

where $x = r/D$, $\langle x^d \rangle$ is the d -th moment of $h(x)$, $\langle x^d \rangle = \int_0^\infty x^d h(x) dx$, and $\Gamma(\cdot)$ is the gamma function. In a perfectly hyperuniform system [1], the non-negative volume coefficient vanishes, i.e., $A = 0$. Perfect crystals and quasicrystals are exactly hyperuniform. Disordered hyperuniform systems can be regarded to possess a "hidden" long-range order [3], and have recently been identified in many materials and systems [4–14]. On the other hand, when $A > 0$ and $B = 0$, the system is *hyposurficial*; examples include homogeneous Poisson point patterns and certain hard-spheres systems [1]. For $A > 0$, the ratio $H = S(0)/S(k_{peak})$, where k_{peak} is the wave number at the largest peak height of $S(\mathbf{k})$, measures qualitatively how close a system is to perfect hyperuniformity. Systems in which $H \lesssim 10^{-3}$ are deemed to be nearly hyperuniform [15].

In this Letter, we quantify the large-scale density fluctuations of amorphous ices modeled via classical molecular dynamics simulations. The samples contain $N = 8192$ water molecules described by the classical TIP4P/2005 interaction potential [16]. Following Ref. [17], we consider low-density amorphous ice (LDA) generated by quenching the liquid at ambient conditions to a temperature of 80 K with a rate of 1 K/ns. We then produce two samples of high-density amorphous ice (HDA) by applying pressure with a rate of 0.01 GPa/ns to LDA and to hexagonal ice (*Ih*) while keeping the temperature constant at $T = 80$ K. We refer to the HDA produced from *Ih* to as HDA_{Ih} , and to the HDA produced from LDA to as HDA_{LDA} . We show that all these amorphs are nearly hyperuniform. In correspondence with the non-equilibrium phase transitions (PTs), structural het-

erogeneities, i.e., molecules in highly distorted local environments, strongly suppress the hyperuniformity and, remarkably, the system becomes hyposurficial. We infer that hyposurficiality is caused by the spatially nearly uncorrelated distribution of clusters of such heterogeneities. We also show that a significant suppression of large-scale density fluctuations emerges when cooling water below the temperature of freezing of the rotational motions, T_{rot} , and we elucidate the connection between molecular rotations and large-scale density fluctuations. T_{rot} is lower than the glass transition temperature T_g at which the translational motions freeze.

To the best of our knowledge, hyposurficiality has never been detected before in any structural transformation. In the present context, it further supports the notion that the LDA-to-HDA transition is first-order-like, consistent with the hypothesized presence of a second critical point in this water model [18, 19]. Our findings shed light on amorphous ices, which play a pivotal role in understanding water properties, and shed also light on structural properties of general glasses. Finally, this work can stimulate experimentalists to probe $S(\mathbf{k})$ at small wave numbers in amorphous systems, and to design experiments to detect large-scale structural order.

Results.— At deeply supercooled conditions, water exhibits polyamorphism, i.e., it exists in more than one amorphous form. The most common forms are LDA and HDA [20–24], and a very high density form has also been proposed to exist at even higher pressures [25]. Amorphous ices have been structurally characterized at short- and intermediate-length-scale [26–28], but no study has probed their large-scale density fluctuations, even though reported experimental $S(\mathbf{k})$'s seem to reach very small values in the limit of $\mathbf{k} \rightarrow 0$ [26, 27].

Figs. 1 (a) and 1 (b) show, respectively, the coefficients A and B during the Ih -to- HDA_{Ih} and LDA-to- HDA_{LDA} transformations. The deviation of A from zero indicates the degree to which the system departs from hyperuniformity in light of its connection with $S(\mathbf{k})$ (Eq. 3). Classical crystals at $T = 0$ K are trivially hyperuniform and, hence, $A = 0$. Our Ih sample acquires slightly larger values, $A \sim 10^{-4}$, because of the finite temperature. A is also low in LDA ($A \sim 10^{-3}$). In correspondence with the non-equilibrium PTs (at $0.85 \lesssim p_T \lesssim 1.0$ GPa in LDA, and at $1.35 \lesssim p_T \lesssim 1.36$ GPa in Ih), A shows a sharp peak, while B drops to almost zero ($\lesssim 10^{-5}$, Fig. 1(b)). We infer that hyposurficiality, as indicated by $B \rightarrow 0$, is due to heterogeneities arranged in clusters distributed in a nearly uncorrelated fashion (Fig. S1 in Supplemental Material). The abrupt change in A and B is a static signature of a first-order-like PT. At high pressures, the predominance of B over A is restored in both HDA_{Ih} and HDA_{LDA} . This suggests that the large-scale density fluctuations are suppressed and are comparable with those in LDA. However, the large-scale structures of HDA_{Ih} and HDA_{LDA} slightly differ one from another at intermediate

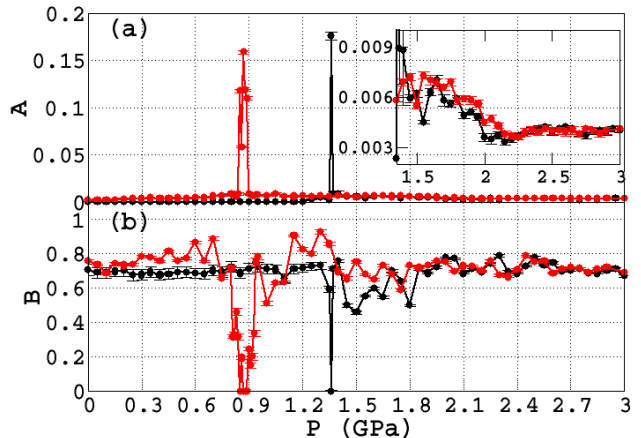


FIG. 1: (a) coefficient A during compression of Ih (black) and LDA (red). Inset: zoom for $1.4 < p < 3.0$ GPa. (b) coefficient B during compression of Ih (black) and LDA (red). The peaks of A signal the Ih -to- HDA and LDA-to- HDA transformations, in correspondence of which the system becomes hyposurficial, as shown by the sharp drop of B .

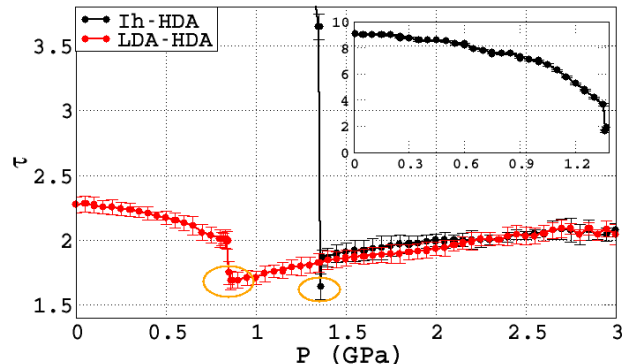


FIG. 2: Translational order metric τ during compression of Ih (black) and LDA (red). Sudden drops of τ occur in correspondence of the PTs. Inset: τ of Ih at low pressures.

pressures, i.e., at $1.5 \lesssim p \lesssim 2.2$ GPa, but upon further compression, the coefficients A of both HDA's become almost identical (Fig. 1, inset), suggesting that HDA_{Ih} and HDA_{LDA} have similar large-scale structures. This observation is further reinforced by the similar values acquired by the coefficient B for both HDA's at $p \gtrsim 2.1$ GPa.

To get deeper insight into the hyposurficiality and hyperuniformity of amorphous ices, we compute the translational order metric τ [3]:

$$\tau = \frac{1}{(2\pi)^3 \rho^2 D^3} \int_0^\infty [S(\mathbf{k}) - 1]^2 d\mathbf{k} \quad (5)$$

where D is a characteristic microscopic length scale. In

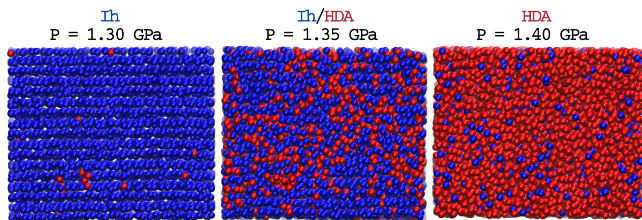


FIG. 3: Snapshots of representative configurations before (left), near (center), and after (right) the Ih -to-HDA transformation. Oxygen sites are represented by blue or red spheres, respectively, for Ih or HDA character based on the local structure index.

the thermodynamic limit, τ diverges for perfect crystals while it vanishes identically for spatially uncorrelated systems. Thus, a deviation of τ from zero, which can only be positive, measures the degree of translational order relative to the fully uncorrelated case. In Fig. 2 we report τ for the compression of Ih (black) and LDA (red). Since Ih possesses long-range order, large positive values of τ for Ih are removed from the main figure and are reported in the inset. This representation allows us to: (i) emphasize the lower values of τ of LDA compared to Ih , and (ii) report the jump in τ in correspondence with both PTs. The finite values of τ for Ih are caused by the finite-size of our sample, which causes a truncation of the upper integration limit in Eq. 5 [38]. For $p < p_T$, τ decreases continuously upon compression in both samples, as structural heterogeneities appear which, at this stage, affect τ but are not concentrated enough to sensitively influence the values of A and of B . In correspondence with the PTs, τ acquires its minimum values, indicating that some degree of decorrelation should be present. Moreover, τ shows a discontinuity, further indication of a first-order-like PT. After the PT, the τ 's of HDA_{Ih} and HDA_{LDA} differ slightly from one another for $1.5 \lesssim p \lesssim 2.2$ GPa. This difference is a further signature of structural differences at the large-scale in HDA_{Ih} and in HDA_{LDA} . Upon further compression, such differences become negligible. Notably, the values of τ for both HDAs at high pressures ($p \sim 3.0$ GPa) are very close to the values of τ in LDA for $0.5 \lesssim p \lesssim 0.8$ GPa. This suggests that similar translational order is present in both amorphous structures, in contrast with the reported differences at small distances [17, 27, 29]. At small length scales, the local environment is tetrahedral with well-separated first and second shells of neighbors in LDA and Ih . By contrast, the environment is distorted in HDA, similar to liquid water at standard conditions, due to interstitial molecules populating the first intershell region [29]. In Fig. 3 we report representative snapshots of the Ih -to-HDA transformation taken before ($p = 1.30$ GPa), in correspondence with ($p = 1.36$ GPa), and after ($p = 1.40$ GPa) the PT. Blue spheres represent Ih sites, red spheres represent HDA environments. The Ih -like

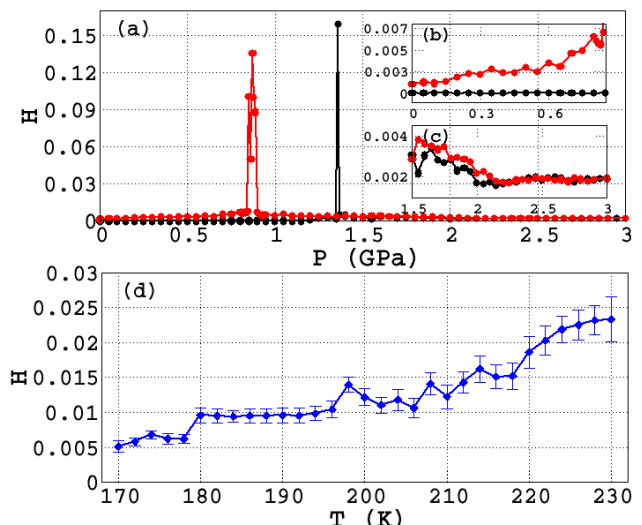


FIG. 4: (a) $H = S(0)/S(k_{peak})$ during compression of Ih (black) and LDA (red). The peaks in correspondence of the PTs (Ih -to-HDA and LDA-to-HDA) reach values that are two orders of magnitude larger than the qualitative threshold for hyperuniformity ($H \sim 10^{-3}$). (b) zoom of H before the LDA-to-HDA PT. (c) zoom of H after the Ih -to-HDA PT. (d) H during cooling of liquid water at $p = 0.1$ GPa (the data are averaged over 10 independent runs).

or HDA-like character is based on the local structure index [30, 31], which quantifies the presence of interstitial molecules in the intershell region. A similar picture holds for the LDA-to-HDA transformation.

We quantify the hyperuniformity of the system by calculating the ratio $H = S(0)/S(k_{peak})$. Fig. 4 (a) reports H for the compression of Ih (black) and LDA (red). Fig. 4 (b) shows that Ih has $H \sim 10^{-4}$ before the PT, and is, therefore, close to perfect hyperuniformity, whereas LDA has H ranging from $\sim 2 \times 10^{-3}$ to $\sim 6 \times 10^{-3}$, signaling that it is nearly hyperuniform. The degree of hyperuniformity continuously decreases with increasing pressure, due to the appearance of HDA-like sites representing structural heterogeneities. In correspondence with the PTs, heterogeneities suppress the hyperuniformity, as indicated by the spikes of H . At $p > p_T$, HDAs are produced and their values of H are shown in Fig. 4 (c). Both HDAs are nearly hyperuniform, with H ranging from $\sim 4 \times 10^{-3}$ to $H \sim 2 \times 10^{-3}$ with increasing pressure. The large scale structures of the two amorphous ices, which differ slightly for $p < 2.2$ GPa, become quite similar above 2.2 GPa. At these high pressures the degree of hyperuniformity of the HDAs is similar to that of LDA at low pressure. Note that LDA and HDA have different hydrogen bond networks (HBNs). The HBN of LDA is dominated by 5-, 6-, and 7-fold rings, in contrast to HDA, whose HBN includes a significant fraction of longer member rings to accommodate the larger density [32]. Despite these differences, each water molecule is almost perfectly four-fold coordinated in LDA and HDA [32]. Therefore,

the nearly hyperuniform nature of LDA and of HDA indicates that the HBNS of both amorphous ices belong to the class of nearly hyperuniform bond networks [8], i.e., isotropic networks lacking of crystallinity and coordination defects, in which all particles are perfectly coordinated, forming continuous random networks -CRNs-, enriched with the suppression of large-scale density fluctuations.

The structure factor of an equilibrium liquid in the infinite-wavelength limit is related to the isothermal compressibility κ_T via $\lim_{\mathbf{k} \rightarrow 0} S(\mathbf{k}) = \rho k_B T \kappa_T$, where ρ is the density and k_B is the Boltzmann constant. The liquid $S(\mathbf{k})$ displays a positive curvature for small wavevectors [33–36]. In our liquid water model at $T = 300$ K $H \sim 0.07$ and progressively decreases with cooling down to the supercooled regime (Fig. 4 (d)). For this model, at the adopted cooling rate, the glass transition occurs at $T_g \approx 200$ K [17]. In the temperature range $196 < T < 204$ K, $H \sim 0.011$ indicating that, in correspondence with the freezing of the translational degrees of freedom, the system is still not hyperuniform. Large-scale density fluctuations keep occurring as the sample is cooled down to $T_{rot} \sim 180$ K [37]. Upon further cooling the large-scale density fluctuations drop rapidly to $H \sim 0.006$ immediately below T_{rot} and then keep decreasing continuously (data not shown) until they saturate at $H \sim 0.002$ for $T \sim 110$ K. We attribute the large-scale density fluctuations for $T_{rot} \lesssim T \lesssim T_g$ mainly to the changes of the HBN caused by the molecular rotations [37], while molecular diffusion is the main contributor for $T > T_g$. The continuous decrease of fluctuations for $T \lesssim T_{rot}$ does not involve any rearrangement of the HBN [37]. It is due instead to small local displacements that reflect the anharmonicity of the potential in the glass and conspire to significantly reduce the large-scale density fluctuations when the CRN is fully formed. Thus, the degree of hyperuniformity is affected by the amplitude of the vibrational motions. The presence of relaxation processes at temperatures well below T_g indicates that LDA is not simply a structurally arrested liquid.

The quantity A/B is the ratio of volume to surface-area fluctuations and is a useful metric to detect the emergence of hyperuniformity or hyposurficiality at thermodynamic conditions away from criticality; at criticality, this ratio becomes meaningless. As shown in Fig. S2 of the Supplemental Material, we find that nearly hyperuniform states occur when $A/B < 0.015$.

Conclusions.— By analyzing the long wavelength density fluctuations of LDA and HDA generated with classical molecular dynamics simulations, we found that both amorphous ices are nearly hyperuniform and have a similar degree of hyperuniformity. This suggests that they should possess similar long-range order in spite of their clear differences at the short- and intermediate-range scales independently of the preparation protocol followed to produce HDA. In correspondence with the transforma-

tion of *Ih*-to-HDA and of LDA-to-HDA, the applied pressure produces clusters of spatially nearly uncorrelated heterogeneities that destroy hyperuniformity. When this occurs, the samples become hyposurficial as density fluctuations that grow like the surface-area of the observation window are absent. Hyposurficiality is a static signature that should be inspected whenever a first-order PT is involved, which, to our knowledge, was never previously observed as a signature of phase coexistence in any context. The sudden appearance of hyposurficiality, the discontinuous profile of the translational order metric τ , and the spike of H in correspondence with the PTs, lead us to conclude that the observed *Ih*-to-HDA and LDA-to-HDA transformations are of the first kind. The first order nature of the LDA-to-HDA metastable phase transition makes conceivable the existence of a second critical point in our model of water.

An additional important finding of our investigation is that the large scale density fluctuations keep decreasing well below T_g and T_{rot} , i.e., well below the temperature of freezing of diffusional and rotational motion, challenging the notion of glasses as kinetically arrested liquids. Our results also indicate that the degree of hyperuniformity of a glass is affected by vibrational motion and, in particular, that not all glasses are hyperuniform.

Finally, we propose that away from criticality, the ratio A/B could provide a useful metric to gauge the degree of volume to surface-area fluctuations, which include hyperuniform and hyposurficial systems at the extremes.

F. M. and R. C. acknowledge the Department of Energy (DOE), grant number DESC0008626

-
- [1] S. Torquato and F. H. Stillinger, Phys. Rev. E **68**, 041113 (2003).
 - [2] C. E. Zachary and S. Torquato, J. Stat. Mech.: Theory and Experiment **2009**, P12015 (2009).
 - [3] S. Torquato, G. Zhang, and F. H. Stillinger, Phys. Rev. X **5**, 021020 (2015).
 - [4] A. Donev, F. H. Stillinger, and S. Torquato, Phys. Rev. Lett. **9**, 09064 (2005).
 - [5] Y. Jiao, T. Lau, H. Hatzikirou, M. Meyer-Hermann, J. C. Corbo, and S. Torquato, Phys. Rev. E **89**, 022721 (2014).
 - [6] L. Pietronero, A. Gabrielli, and F. S. Labini, Physica A **306**, 395 (2002).
 - [7] R. Xie, G. G. Long, S. J. Weigand, S. C. Moss, T. Carvalho, S. Roorda, M. Hejna, S. Torquato, and P. J. Steinhardt, Proc. Natl. Acad. Sci. USA **110**, 13250 (2013).
 - [8] M. Hejna, P. J. Steinhardt, and S. Torquato, Phys. Rev. B **87**, 24504 (2013).
 - [9] M. Florescu, S. Torquato, and P. J. Steinhardt, Proc. Natl. Acad. Sci. USA **49**, 20658 (2009).
 - [10] W. Man, M. Florescu, E. P. Williamson, Y. He, S. R. Hashemizad, B. Y. C. Leung, D. R. Liner, S. Torquato, P. M. Chaikin, and P. J. Steinhardt, Proc. Natl. Acad. Sci. USA **110**, 15886 (2013).
 - [11] G. Zito, G. Rusciano, G. Pesce, A. Malafronte, R. D.

- Girolamo, G. Ausanio, A. Vecchione, and A. Sasso, Phys. Rev. E **92**, 050601(R) (2015).
- [12] A. Chremos and J. F. Douglas, Annalen der Physik p. 1600342 (2017), 1600342.
- [13] G. Zhang, F. H. Stillinger, and S. Torquato, Sci. Rep. **6**, 36963 (2016).
- [14] T. Goldfriend, H. Diamant, and T. A. Witten, Phys. Rev. Lett. **118**, 158005 (2017).
- [15] S. Atkinson, G. Zhang, A. B. Hopkins, and S. Torquato, Phys. Rev. E **94**, 012902 (2016).
- [16] J. L. F. Abascal and C. Vega, J. Chem. Phys. **123**, 234505 (2005).
- [17] J. Wong, D. A. Jahn, and N. Giovambattista, J. Chem. Phys. **143**, 074501 (2015).
- [18] J. L. F. Abascal and C. Vega, J. Chem. Phys. **133**, 234502 (2010).
- [19] R. S. Singh, J. W. Biddle, M. A. Anisimov, and P. G. Debenedetti, J. Chem. Phys. **144**, 144504 (2016).
- [20] P. G. Debenedetti, J. Phys.: Condens. Matter **15**, R1669 (2003).
- [21] T. Loerting and N. Giovambattista, J. Phys.: Condens. Matter **18**, R919 (2006).
- [22] O. Mishima and H. E. Stanley, Nature **396**, 329 (1998).
- [23] T. Loerting, V. Fuentes-Landetea, P. H. Handlea, M. Seidl, K. Amann-Winkel, C. Gainaru, and R. Bohme, J. Non-Cryst. Solids **407**, 423430 (2015).
- [24] K. Amann-Winkel, R. Bohmer, F. Fujara, C. Gainaru, B. Geil, and T. Loerting, Rev. Mod. Phys. **88**, 011002 (2016).
- [25] T. Loerting, C. Salzmann, I. Kohl, E. Mayer, and A. Hallbrucker, Phys. Chem. Chem. Phys. **3**, 5355 (2001).
- [26] C. A. Tulk, C. J. Benmore, L. Urquidi, D. D. Klug, J. Neufeing, B. Tomberli, and P. A. Egelstaff, Science **297**, 1320 (2002).
- [27] J. L. Finney, A. Hallbrucker, I. Kohl, A. K. Soper, and D. T. Bowron, Phys. Rev. Lett. **88**, 225503 (2002).
- [28] K. Winkel, E. Mayer, and T. Loerting, J. Phys. Chem. B **115**, 1414114148 (2011).
- [29] A. K. Soper and M. A. Ricci, Phys. Rev. Lett. **84**, 2881 (2000).
- [30] E. Shiratani and M. Sasai, J. Chem. Phys. **104**, 7671 (1996).
- [31] E. Shiratani and M. Sasai, J. Chem. Phys. **108**, 3264 (1998).
- [32] R. Martoňak, D. Donadio, and M. Parrinello, J. Chem. Phys. **122**, 134501 (2005).
- [33] J. A. Sellberg, C. Huang, T. A. McQueen, H. L. N. D. Loh, D. Schlesinger, R. G. Sierra, D. Nordlund, C. Y. Hampton, D. Starodub, D. P. DePonte, et al., Nature **510**, 381 (2014).
- [34] K. T. Wikfeldt, A. Nilsson, and L. G. M. Pettersson, Phys. Chem. Chem. Phys. **13**, 19918 (2011).
- [35] D. Dhabal, K. T. Wikfeldt, L. B. Skinner, C. Chakravarty, and H. K. Kashyap, Phys. Chem. Chem. Phys. **19**, 3265 (2016).
- [36] G. N. I. Clark, C. R. Cappa, J. D. Smith, R. J. Saykally, and T. Head-Gordon, Mol. Phys. **108**, 1415 (2010).
- [37] F. Martelli, H.-Y. Ko, E. C. Oğuz, and R. Car, arXiv:1609.03123 [physics.comp-ph] (2016).
- [38] The upper integration limit is defined by the reciprocal vectors associated to the natural periodicity of I_h in units of the reciprocal lattice vectors of the sample supercell.

Supplementary Material for: Large-scale structure and hyperuniformity of amorphous ices

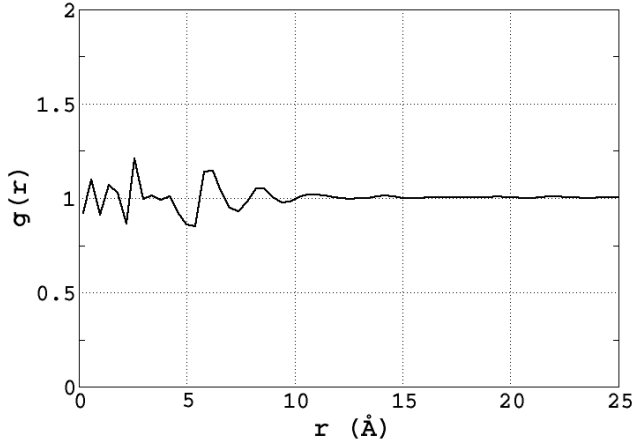
Fausto Martelli¹, Salvatore Torquato^{1,2}, Nicolas Giovambattista^{3,4}, Roberto Car^{1,2}

¹*Department of Chemistry, Princeton University, Princeton NJ, USA*

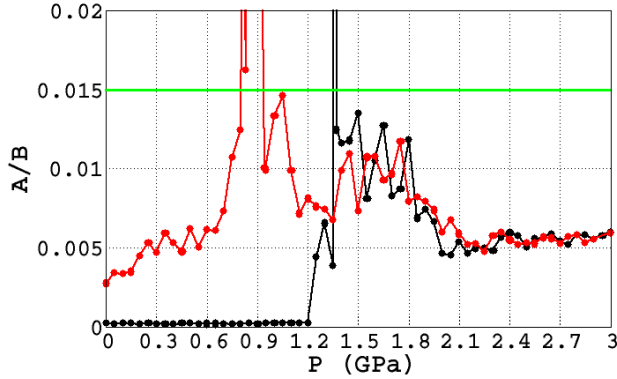
²*Department of Physics, Princeton University, Princeton NJ, USA*

³*Department Physics, Brooklyn College of the City University of New York, New York, NY, USA*

⁴*Ph.D. Programs in Chemistry and Physics, The Graduate Center of the City University of New York, New York, New York 10016, USA*



S 1: Radial distribution function of the centers of mass of the heterogeneous clusters. Here we consider clusters of red spheres (see center panel of Fig.3). A cluster contains at least two neighboring sites of same character. A similar figure could have been drawn using the blue spheres in Fig.3.



S 2: Ratio A/B during compression of Ih (black) and LDA (red). In correspondence with the structural transformations of Ih and LDA to HDA, the ratio A/B peaks at very high values of $\sim 10^4$, i.e. well outside the range of the figure where only values of A/B up to 0.02 are reported. The horizontal green line indicates a qualitative threshold below which a system can be considered to be approximately hyperuniform. The value of A/B fluctuates near ~ 0.0002 for Ih , while it fluctuates near ~ 0.005 for LDA and HDA away from the regions containing a larger fraction of heterogeneities below and above the peaks associated to the structural transformations. We speculate that it should be possible to prepare amorphs with higher degree of hyperuniformity with e.g. protocols having slower cooling/pressurizing rates.